

Heart Failure Readmission Prediction Using Seismocardiogram Signal

Rajkumar Dhar¹, Rakib Hossen¹, Peshala T Gamage¹, Richard H Sandler¹, Nirav Y Raval¹, Robert J Mentz¹, and Hansen A Mansy¹

¹Affiliation not available

March 06, 2024

Abstract

Heart failure (HF) is considered a global pandemic because of increasing prevalence, high mortality rate, frequent hospitalization and associated economic burden. This study explores a noninvasive method that may help in managing HF patients by predicting HF readmission. Methods: Seismocardiogram (SCG) signal is the low frequency chest vibration produced by the mechanical activity of heart. SCG signal was acquired from 101 patients with HF including in those readmitted to the hospital during the study period. Features were extracted from SCG signals. Several conventional machine learning (ML) models were developed using selected SCG and heart rate variability features. Furthermore, SCG signals were transformed into images using a time-frequency distribution method. Images were used to train a deep learning model. The models were able to predict the readmission status of the HF patients. Results: ML algorithms achieved higher accuracy than the deep learning model in classifying the readmitted and non-readmitted HF patients. K-nearest neighbor (KNN) achieved the highest classification accuracy (89.4% accuracy, 87.8% sensitivity, and 90.1% specificity). The study results suggest that SCG signal may be useful for readmission prediction of HF patients. Significance: Use of SCG signal may help the management of HF patients and improve their quality of life.

Heart Failure Readmission Prediction Using Seismocardiogram Signal

Rajkumar Dhar, Md Rakib Hossen, Peshala T. Gamage, Richard H. Sandler, Nirav Y. Raval, Robert J. Mentz, Hansen A. Mansy

Abstract— Objective: Heart failure (HF) is considered a global pandemic because of increasing prevalence, high mortality rate, frequent hospitalization and associated economic burden. This study explores a noninvasive method that may help in managing HF patients by predicting HF readmission. **Methods:** Seismocardiogram (SCG) signal is the low frequency chest vibration produced by the mechanical activity of heart. SCG signal was acquired from 101 patients with HF including in those readmitted to the hospital during the study period. Features were extracted from SCG signals. Several conventional machine learning (ML) models were developed using selected SCG and heart rate variability features. Furthermore, SCG signals were transformed into images using a time-frequency distribution method. Images were used to train a deep learning model. The models were able to predict the readmission status of the HF patients. **Results:** ML algorithms achieved higher accuracy than the deep learning model in classifying the readmitted and non-readmitted HF patients. K-nearest neighbor (KNN) achieved the highest classification accuracy (89.4% accuracy, 87.8% sensitivity, and 90.1% specificity). The study results suggest that SCG signal may be useful for readmission prediction of HF patients. **Significance:** Use of SCG signal may help the management of HF patients and improve their quality of life.

Index Terms—Biomedical signal processing, Biomedical acoustics, Congestive heart failure, Machine learning, Feature extraction, Convolutional neural networks.

Manuscript submitted on February 14, 2024. This study was supported by NIH grant R44HL099053. Richard H. Sandler and Hansen A. Mansy are part owners of Biomedical Acoustics Research Company, which is the primary recipient of the NIH grant R44HL099053, as such they may benefit financially because of the outcomes of the research work reported in this publication.

Rajkumar Dhar is with the Department of Mechanical and Aerospace Engineering, University of Central Florida, Orlando, FL 32816 USA (e-mail: rajkumar.dhar@ucf.edu).

Md Rakib Hossen, Richard H. Sandler and Hansen A. Mansy are with the Department of Mechanical and Aerospace Engineering, University of Central Florida, USA.

Peshala T. Gamage is with the Department of Biomedical Engineering and Science, Florida Tech, USA.

Nirav Y. Raval is with Advent Health, USA.

Robert J. Mentz is with the Department of Medicine, Duke University, USA.

I. INTRODUCTION

Heart failure (HF) is a chronic progressive medical condition marked by the diminished capacity of the heart to effectively pump blood. HF is a major global health concern and considered a pandemic with an estimated 64 million cases worldwide [1] and 6 million in the United States [2]. This is projected to rise to 8.5 million in 2030 in the US [3]. This increasing prevalence mainly accounts for the aging populations who are at greater risk of developing HF. Advances in medical diagnosis and treatment have improved survival rates prolonging life in individuals with HF [1]. Nevertheless, the mortality rate related to HF is still excessively high. A meta-analysis by Jones et al. in 2018 showed that the 1 and 5-year survival rate of HF is 86.5% and 56.7%, respectively [4]. According to a more recent study by Bozkurt et al., 28% of 263,525 patients died during the first year of first HF hospitalization [3]. Apart from this, the economic burden related to HF is also staggering [5]. The total cost for HF was estimated at \$43.6 billion in the US, which is projected to increase to \$70 billion by 2030 [6], [7]. The main driver of HF healthcare cost is hospitalization [8] as HF is associated with a very high number of hospital readmission rate. After discharge, about 25% and 50% of HF patients are readmitted within the 30 days and 6 months period, respectively [2], [9]. With the increase of HF prevalence, the readmission rate and associated cost are likely to be increased in the coming years. Therefore, early readmission prediction may allow interventions that may reverse patient deterioration and avoid readmission.

HF can be classified based on left ventricular ejection fraction (LVEF). LVEF is the fraction of blood pumped out of heart's left ventricle (LV) during systole. It provides a measurement of LV systolic function which is responsible for ejecting oxygenated blood from the heart to the rest of the body. Normal range of LVEF is 50-70% [10]. Classification of HF regarding LVEF is illustrated in Table I.

TABLE I
CLASSIFICATION OF HF ACCORDING TO LVEF

HF class	LVEF
HFrEF	$\leq 40\%$
HFmrEF	41-49%
HFpEF	$\geq 50\%$

Here, HFrEF is HF with reduced ejection fraction, HFmrEF is HF with mildly reduced ejection fraction, and HFpEF is HF with preserved ejection fraction [6]. LVEF stands for left ventricular ejection fraction.

HFrEF comprises approximately 50% of total HF cases [11]. Patients with HFrEF have a higher mortality rate than HFpEF [12], [13]. Although all-cause readmission is higher in HFpEF, HF readmission is higher in HFrEF [14]. In addition, the cost of readmission is higher in HFrEF patients [15]. Regardless of the HF class, the high readmission rate is avoidable with preventive measures [16]. In [17], it was demonstrated that a post-discharge transitional care program can greatly reduce the HF readmission rate and the associated cost. Taking this into account, continuous efforts have been made to build an early and reliable HF readmission prediction model that may help the clinicians to make timely targeted interventions to prevent readmissions.

Electronic health records (EHR) and wearable sensors are the main data sources that have been used to predict HF readmission. EHR includes patient demographics, medications, vital signs, medical history, laboratory data etc. With wearable devices measures including intrathoracic impedance, electrocardiogram (ECG), and seismocardiogram (SCG) can be acquired and used as predictors of HF readmission. The predictive accuracy values of these studies are widely varied. In [18], authors used EHR data and achieved 83.19% accuracy in 1068 patients. In another study, sensitivity, and specificity of 48% and 70% are achieved respectively using medical data of 10757 HF patients [19]. A review article by Liu et al. showed that B-type natriuretic peptide (BNP) and N-terminal pro-brain natriuretic peptide (NT- proBNP) are the most used predictors from the EHR data [20].

Other authors used sensor data to predict HF readmission. Intrathoracic impedance-based models obtained variable predictive accuracy ranging from 21-76% suggesting the uncertainty in predicting HF readmission [21], [22], [23], [24]. In [23], ECG, skin impedance, temperature etc. were acquired from 100 patients at home with a multisensory patch for 3 months. High prediction accuracy was achieved (sensitivity=86%, specificity=87.5%) using the sensor data, although the study required baseline data for analysis. Boehmer et al. used defibrillators implanted in patients to acquire data to predict hospitalization [25]. Invasive accelerometer-acquired heart sounds (similar to SCG), heart rate, intrathoracic impedance, respiration rate and tidal volume data were collected from the implanted device which were able to alert clinicians before HF hospitalization (sensitivity=70%). In another SCG-based study Lin et al. identified HF patients by calculating LVEF from SCG and ECG signals [26]. In the study 40 subjects were enrolled (25 HF and 15 healthy). Ratio of pre-ejection period and left ventricular ejection time was calculated from SCG and ECG signals which was found inversely proportional to LVEF (correlation coefficient 0.73). A threshold ratio of 0.33 distinguished HF from healthy participants with 96% accuracy (sensitivity 98% and specificity 94%). Inan et al. used SCG signal to distinguish between compensated and decompensated HF patients [27]. The patients needed to perform the 6-minute walk test (6MWT) in this study. Similarity between SCG signals before and after the test was used as a metric to differentiate the two groups. Higher

similarity was found in decompensated patients suggesting their reduced cardiovascular reserve. Although the above studies had several limitations such as requiring baseline data, demanding patients to perform 6MWT or using invasive measurements, these studies demonstrated the merit of SCG signal in predicting HF readmission. The current study investigates the feasibility of using SCG and ML for HF readmission prediction when baseline measurements are not available.

II. MATERIALS AND METHOD

A. Data Acquisition:

The dataset used in this study was collected at AdventHealth Orlando after IRB approval by the University of Central Florida (protocol number: BIO-16-12783, the date of approval: March 6, 2023). HF patients were recruited after their discharge from the hospital. Overall, 101 patients were included in this study. Data were acquired in single or multiple sessions per patient. After data quality inspection, 24 recording sessions were excluded due to poor quality of the acquired signal(s). This resulted in the exclusion of 20 patients from the study. Data analysis was performed in the remaining 81 patients (19 females, 75 HFrEF and 6 HFpEF) who had total 142 sessions. After the initial discharge, 22 patients (who attended 41 recording sessions) were readmitted to the hospital during the window of data acquisition (six month). The protocol included 3 minutes of data acquisition in each session when patients were sitting on a 45-degree inclined exam table with their legs extended. The following three signals were acquired from the patients:

- i. Seismocardiography (SCG): Acquired using a tri-axial accelerometer (Model: 356A32, PCB Piezotronics, Depew, NY) placed on the chest surface at the 4th intercostal space near the left lower sternal border. Signal was amplified using a signal conditioner (Model: 482C, PCB Piezotronics, Depew, NY) with a gain of 100. The x, y and z components of the accelerometer are pointed toward lateral (left to right), caudocranial (head to toe) and dorsal-ventral (normal to chest surface) directions, respectively. This study includes the analysis of z-axis of the accelerometer.
- ii. Electrocardiography (ECG): Acquired by IX-B3G bio-potential recorder (iWorx Systems, Inc., Dover, NH).
- iii. Galvanic skin response (GSR): Provides an estimate of lung volume [28]. Acquired by IX-B3G bio-potential recorder.

All the signals were acquired at a sampling rate of 10 kHz.

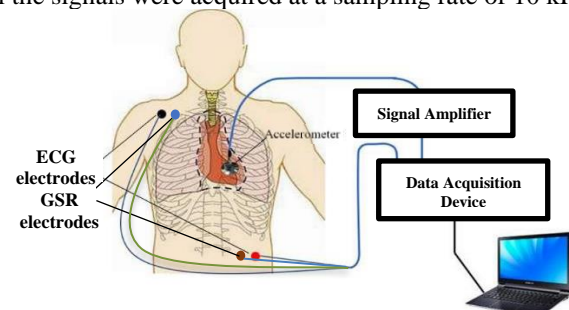


Fig. 1. Schematic of experiment setup.

B. Data Analysis:

Overview: The workflow diagram of data analysis is shown in Fig. 2. The process started with filtering raw signals (band pass = 0.5 to 100 Hz), followed by the segmentation of SCG and ECG signals[29]. After that SCG beats were clustered using unsupervised clustering method (k-medoid clustering) [30]. The clustering was correlated to the respiration phases which were obtained from GSR signal. This clustering provides a medoid SCG beat for each cluster. Clustering features (described below) were extracted using the relationship between the medoid SCG beats and rest of the SCG beats. Other time- and frequency-domain features were extracted from the cluster “representative” beats (described below). Conventional machine learning models were trained and tested using selected SCG features along with few heart rate variability (HRV) features. This concludes the first approach of analysis that utilizes conventional ML.

In the second approach, few SCG beats (3-5) that were closest (in terms of waveform shape) to the medoid beats were transformed into images using a time-frequency distribution method (polynomial chirplet transform or PCT). The images were fed to a CNN model for training and testing.

1) Preprocessing:

After visually checking the signal quality, noisy portions of the data were discarded. This noise mainly came from patient movements. The Rest of the data (usually 100 to 140 seconds) was considered for analyzing. The raw ECG, SCG and GSR signals were down sampled to 1kHz. After that, ECG and SCG signals were forward-backward filtered using a 4th order Chebyshev type 2 bandpass filter with cutoff frequencies of 0.5 and 100 Hz. GSR signal was detrended and a flow rate signal was calculated by differentiating the GSR signal.

2) Segmentation and normalization:

The R-peaks of the ECG signal was detected using Pan Tompkins algorithm (Tompkins, 1985). SCG and ECG beats were chosen to start 0.1 second before ECG R-wave and end 0.1 second before the next R-wave. After segmentation, each SCG beat was normalized by its peak-to-peak amplitude.

3) Unsupervised clustering (k-medoid clustering):

Studies on SCG signals [30], [31], [32] reported that SCG signal has morphological variability. The clusters of similar SCG beats were found to correlate with the respiration phases. It was suggested that clustering SCG beats into two clusters optimally lowers the variability and make the feature extraction more accurate [30]. To group the SCG beats with close morphological features, k-medoid clustering method was used. The unsupervised clustering method requires two initial beats. Efficient clustering depends on good initialization. In the current study, the SCG beats are initially divided into two groups based on either lung volume (high and low) or flow rate (high and low). SCG beats are considered to be more similar when the distance between them is smaller. Dynamic time warping (DTW) and cross correlation methods are the two methods chosen to measure the distance (i.e. morphological dissimilarity) between the SCG beats. After dividing the beats into two groups based on lung volume and flow rate, center beats were chosen from each group which had the minimum sum of distances with its neighboring beats in the same group. These two center beats are chosen as the initial beats for the k-medoid method which is named as initial medoids.

After obtaining the initial medoids the clustering process began. The algorithm continued to update the cluster medoids by calculating the sum of distances and then update the

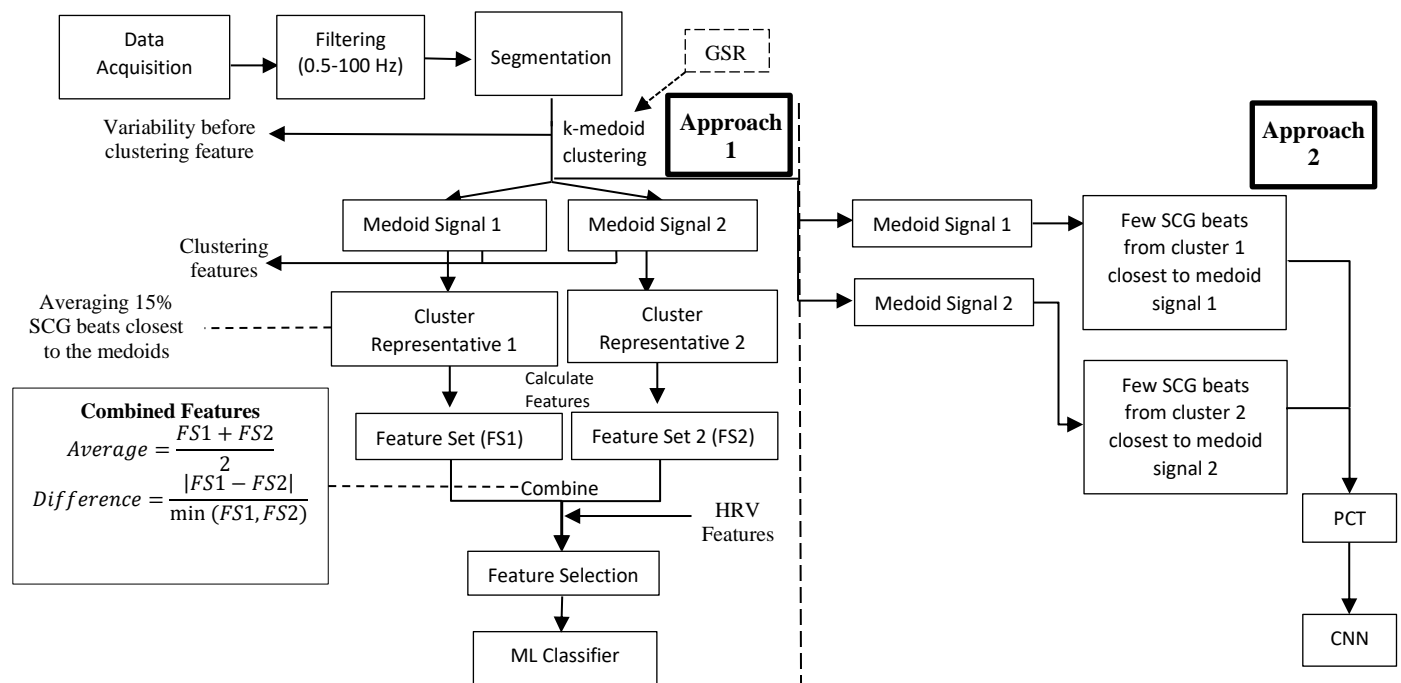


Fig. 2. Flow diagram of data analysis.

clusters by grouping the beats that have morphological similarities measured by DTW distance. The algorithm stopped when there was no change in the assignment of the SCG beats to the clusters in two consecutive iterations. As there were two bases of grouping (lung volume and flow rate) and two distance measuring methods (DTW and cross correlation), all the four combinations of getting the initial medoids were performed. The combination that produced the

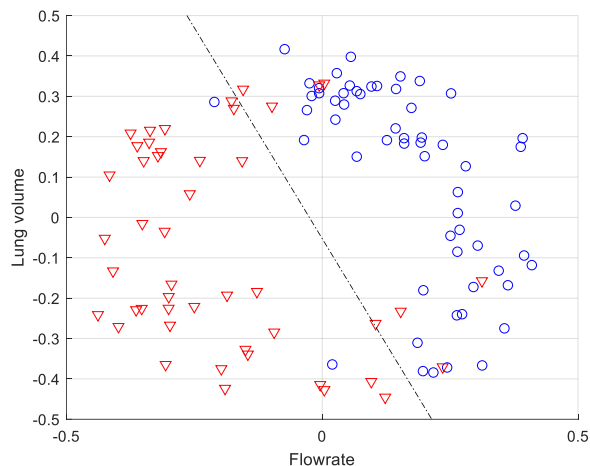


Fig. 3. k-medoid clustering of SCG beats of a representative recording session (Subject 25, 3rd session) in lung volume-flowrate space. Blue circles and red triangles are the beats of the two clusters. A decision boundary (dashed line) is plotted to show the clear separation between the two clusters.

most optimum clustering of SCG beats was selected. Clustering quality was also checked by plotting the clustered beats in a lung volume-flow rate space (Fig. 3). A decision boundary was drawn to visualize the separation of the beats into two clusters.

After getting the cluster medoids, 15% SCG beats that are closest (measured by DTW distance) to the medoid signal in a cluster were averaged to create a SCG beat that is a representative of that cluster. Features were extracted from both cluster medoids and cluster representatives.

4) Feature Extraction and Selection:

In total, 63 SCG features were extracted. These include clustering, time- and frequency-domain features. In addition, 8 HRV features were added to complete the feature set. Random forest (RF) algorithm was employed for feature selection. RF is a popular and powerful algorithm which falls under embedded feature selection method. This embedded method combines the benefits of other two feature selection methods (filter and wrapper) by allowing interaction with the classifier (like wrapper method) and being computationally lighter at the same time producing better classification results [33], [34]. 11 features were selected (7 SCG and 4 HRV features). A list of selected features is given in Table II.

5) Image construction using time-frequency conversion:

For deep learning approach (approach 2 in Fig. 2) PCT (a time frequency distribution) of the SCG signals was calculated and resulted in images. Depending on the length of session

data, 3-5 SCG beats closest (as measured by DWT) to the medoid signals were processed by PCT. This resulted in 2D images with time and frequency information in horizontal and vertical axis, respectively (Fig. 4(b)). The PCT coefficient values were presented using ‘Parula’ colormap. PCT is found to be more suited than other TFD methods for SCG and heart sound related studies [35], [36].

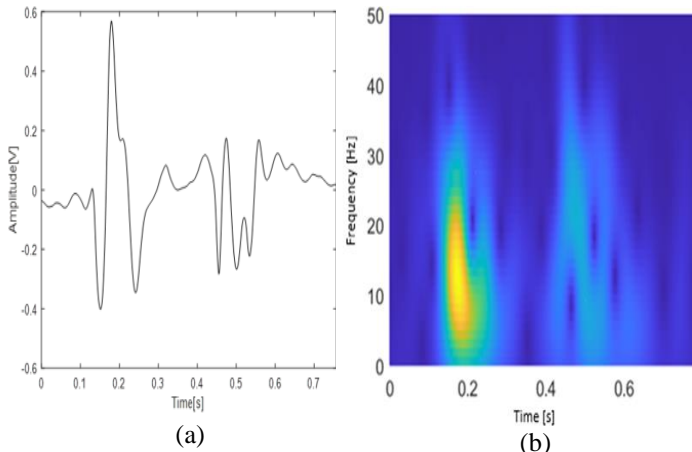


Fig. 4. (a) SCG medoid beat of a representative subject (subject 3, session 3), and (b) the corresponding time-frequency distribution coefficient heatmap as calculated by PCT.

6) Conventional ML algorithms:

Three different ML algorithms were employed to evaluate the efficacy of the feature set in predicting HF readmission. These methods are k-nearest neighbor (KNN), multilayer perceptron neural network (MLP-NN) and extreme gradient boosting (XGBoost). The hyperparameters were tuned to maximize the model performance. Since there was imbalance in the number of observations between the two classes, the decision threshold governing the conversion of the prediction probability to a class label was shifted from the default value of 0.5 and tuned to 0.7 to maximize sensitivity. The leave-one-subject-out cross validation approach was used for testing to avoid subject bias.

7) Convolutional Neural Network:

For image classification, the Residual-networks (ResNet-34) model was used. ResNets are being widely used in image classification after introduced by He et al. [37]. Several ResNet-based time-frequency image classification tasks have been studied previously [20], [38], [39].

In this study, a 34-layer CNN network, ResNet-34 was used. Images were resized to 224 by 224 pixels with nearest neighbor interpolation to match the input requirement of ResNet-34. Adam optimizer with learning rate 0.000008 was chosen. Cross-entropy loss metric was used for performance measurement. The number of epochs was 30 with a batch size of 8.

TABLE II
SELECTED FEATURES

Feature Index	Feature Name	Description	
1	Intra-session waveform variability before clustering (WV_{bc}).	The dissimilarity among the SCG beats within a session. Dissimilarity was calculated using dynamic time warping (dtw) distance. $WV_{bc} = \frac{1}{n} \sum_{i=1}^n \frac{dtw(C, X_i)}{l_i}$ C : medoid beat before clustering, X_i : i th SCG beat, l_i : warping path length, n = number of SCG events in a session.	SCG Features
2	Inter-cluster waveform variability (WV_{inter})	Average dissimilarity between the medoid of a cluster and SCG beats of the other cluster. $WV_{inter} = \frac{1}{n_1+n_2} \left[\sum_{i=1}^{n_1} \frac{dtw(C_1, X_{i2})}{l_i} + \sum_{i=1}^{n_2} \frac{dtw(C_2, X_{i1})}{l_i} \right]$ n_1, n_2 : number of events in Cluster 1 and 2, C_1, C_2 : SCG medoid of cluster 1 and 2, X_{i1}, X_{i2} : i th SCG event of cluster 1 and 2	
3	Intra-cluster waveform variability (WV_{intra})	Average dissimilarity between the medoid and SCG beats of the same cluster. $WV_{intra} = \frac{1}{n_1+n_2} \left[\sum_{i=1}^{n_1} \frac{dtw(C_1, X_{i1})}{l_i} + \sum_{i=1}^{n_2} \frac{dtw(C_2, X_{i2})}{l_i} \right]$	
4	Average RMS amplitude of instantaneous frequency (F_{ins})	Instantaneous frequency (F_{ins}) was calculated as the frequency first moment of the time-frequency distribution (PCT), normalized by the integral of PCT at that time instant. $F_{ins} = \frac{\int_{0.5}^{50} f * PCT(t, f) df}{\int_{0.5}^{50} PCT(t, f) df}$ Then, the RMS of F_{ins} was calculated over the duration of the beats under consideration.	
5	Average turning point ratio (TPR)	$TPR = \frac{N((x_i - x_{i-1}) * (x_i - x_{i+1})) > 0}{length\ of\ the\ signal}$ Quantification of the randomness in a time-series signal.	
6	Average sample entropy (SmEn)	$SmEn = -\ln \frac{count_{m+1}(similar)}{count_m(similar)}$; here denominator and numerator are the number of matched template pairs of length m and $m+1$ in the waveform, respectively [40].	
7	Average Higuchi dimension (D_H)	Measures the irregularity in a time-series signal [41].	
8	Low frequency power (LFP)	Spectral power of heart rate (HR) in .04-.15 Hz frequency band.	HRV Features
9	High frequency power (HFP)	Spectral power of HR in .15-.4 Hz frequency band.	
10	Total Power (TP)	Total spectral power of HR in 0-0.4 Hz frequency band.	
11	pNN50	Proportion of successive RR intervals that differ by more than 50 ms.	

Selected SCG (1-7) and HRV (8-11) features are provided with short descriptions. The features (4-7) are obtained by averaging the features from the two cluster representative waveforms (for each recording session).

Keeping in mind that training a CNN model takes considerable amount of time, 38 patients (21 readmitted) with 90 sessions were trained and tested in leave-one-subject-out manner. Due to the low number of readmitted patients, almost all of them (21 out of 22) were included in the subset of 38 patients to facilitate the learning. The number of observations for both classes (readmitted and non-readmitted) was balanced in this subset by random undersampling the majority class (non-readmitted patients). The remaining 43 patients (1 readmitted) with 52 sessions were only used for testing. These patients were tested using a model trained by the data from all the sessions of the 38 patients. The performance metrics were determined encompassing all the 81 patients. This also mimics a real-life application of the developed deep learning model

where the model is trained using the available HF patient data and the trained model predicts the readmission of the future HF patients.

III. RESULTS

Three metrics were used to show the results (Equation 1-3).

$$sensitivity = \frac{True\ positive\ (TP)}{True\ positive\ (TP) + False\ negative\ (FN)} \quad (1)$$

$$specificity = \frac{True\ negative\ (TN)}{True\ negative\ (TN) + False\ positive\ (FP)} \quad (2)$$

$$accuracy = \frac{TP + TN}{TP + TN + FP + FN} \quad (3)$$

The obtained results are presented in Table III.

TABLE III
MODEL PERFORMANCE

Model	Sensitivity	Specificity	Accuracy
KNN	0.878	0.901	0.894
MLP-NN	0.878	0.812	0.831
XGBoost	0.854	0.802	0.817
ResNet-34	0.805	0.811	0.810

These results suggest that conventional ML algorithms performed better than deep neural network model with higher sensitivity. Specially, KNN outperformed other models with close to 90% accuracy.

IV. DISCUSSION

A non-invasive approach of predicting HF readmission was proposed and tested in this study. The linear acceleration in dorsal-ventral direction was analyzed and used to classify HF patients (admitted vs. non-readmitted). Data analysis was performed in two different approaches: (a) conventional machine learning and (b) deep learning. In the first approach features were first extracted from SCG beats and heart rate variability. Feature selection was performed followed by using three different ML algorithms. For the second approach, time-frequency distribution (PCT) was applied to convert the time-domain signal into a 2D image with time and frequency information. The images were resized and fed into a CNN network (ResNet-34) for classification.

Results showed that handcrafted features provided better accuracy than the CNN method. One reason for this can be the inclusion of heart rate variability features in the feature set which wasn't provided to CNN model. Given the higher performance of conventional ML models (with the SCG and

HRV features), a discussion of these features that correlate those with HF conditions may be useful. The focus here will be given to SCG clustering features and HRV features.

The first three features in Table II are the SCG clustering features. The first feature is intra-session waveform variability calculated before clustering. This feature represents the dissimilarity among SCG beats during a session. Inter- and intra-cluster variability features were also obtained after clustering. These features present the average dissimilarity of SCG beats between and within the clusters, respectively. Overall, these clustering features indicate the beat-to-beat waveform variability. The distributions of the clustering feature values in non-readmitted and readmitted patient groups are shown in Fig. 5. For comparison, feature values of a group of 14 healthy subjects are also shown. Data was acquired from the healthy subjects using the same protocol.

Heart failure is associated with chronic sympathetic/parasympathetic imbalance resulting in increased sympathetic and decreased parasympathetic drive [42], [43], [44], [45]. This also decreases peripheral acetylcholine (ACh) secretion [46]. ACh is the main neurotransmitter of the parasympathetic nervous system [47]. Binding inhibition of ACh to receptors in heart has several effects such as increasing heart rate and heart contraction force, etc. [48], [49]. In fact, increasing ACh might be a logical HF treatment [46], [50] since it may reverse the effect of decreased ACh with HF.

Heart failure is associated with chronic sympathetic/parasympathetic imbalance resulting in increased sympathetic and decreased parasympathetic drive [42], [43], [44], [45]. This also decreases peripheral acetylcholine (ACh) secretion [46]. ACh is the main neurotransmitter of the parasympathetic nervous system [47].

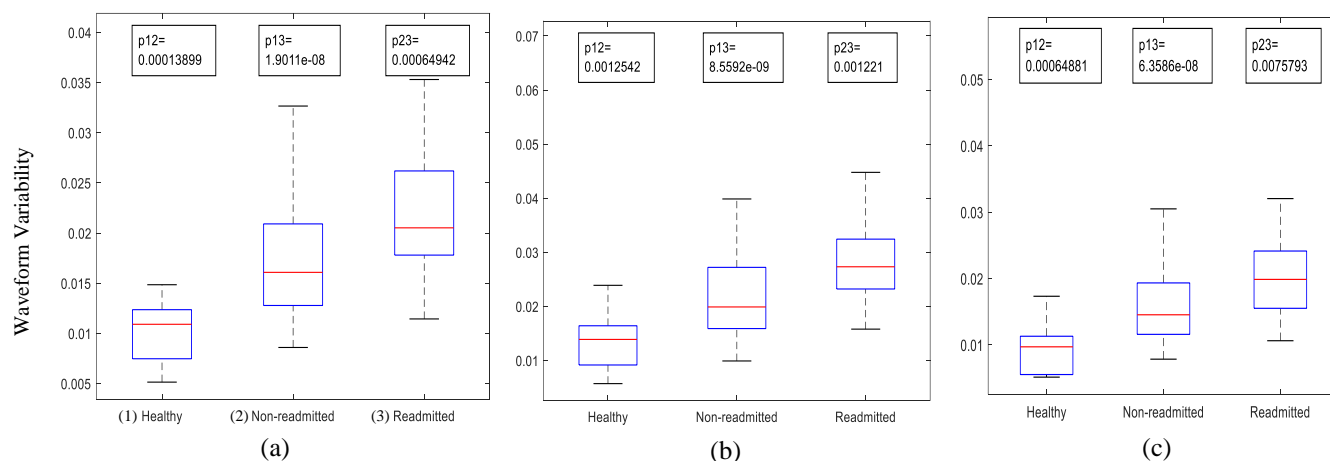


Fig. 5. shows the feature values of (1) healthy, (2) non-readmitted and, (3) readmitted groups in boxplot for (a) intra-session waveform variability before clustering, (b) inter-cluster variability and (c) intra-cluster variability features. All the feature values are highest in readmitted patient group and lowest in the healthy group. The differences between each pair of the groups are statistically significant as depicted by p-values (two-sample t-test) at the top of each image. Here, the numbers beside 'p' indicate the numbers of the groups being compared (1-Healthy, 2-non-readmitted groups, 3-readmitted).

Binding inhibition of ACh to receptors in heart has several effects such as increasing heart rate and heart contraction force, etc. [48], [49]. In fact, increasing ACh might be a logical HF treatment [46], [50] since it may reverse the effect of decreased ACh with HF.

The trend of increased beat-to-beat SCG waveform variability with worsened heart failure (see Fig. 5) may be explained by the decreased acetylcholine (ACh) release in HF. In an animal study Ahammer et al. reported that decreased ACh increased beat-to-beat contraction strength variability of murine atrial preparation [51]. In that study hearts were removed, and the atria were dissected from the ventricles. Variability analysis of contraction strengths was performed under control and ACh treated conditions. Variability of contraction strength was significantly higher in control tissue (which had lower ACh). This suggests that decreased ACh in HF may play a role in increasing the beat-to-beat variability of cardiac contraction. Increased cardiac contraction variability (associated with decreased ACh secretion) is believed to be a major contributor to SCG signal variability [52], [53]. The lowest variability found in healthy group (Fig. 5) further strengthens this argument.

Another important factor to be considered here is the trend in HRV features. Fig. 6 shows the boxplots of selected HRV features for the 3 groups of subjects.

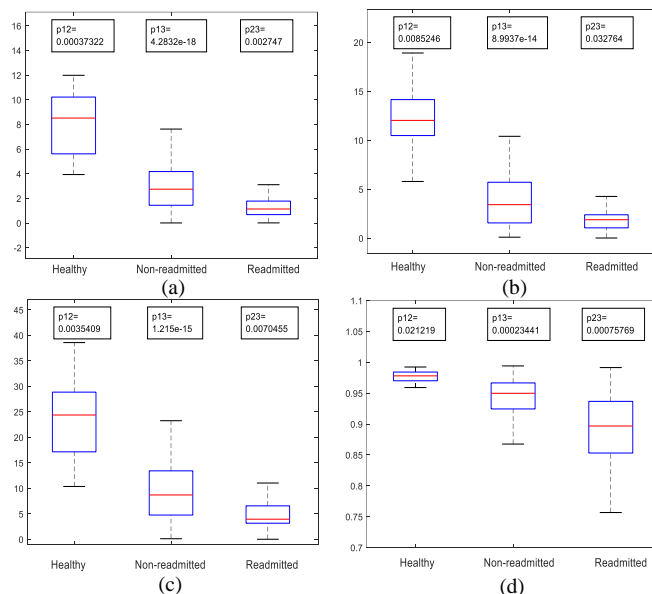


Fig. 6. shows the feature values of (1) healthy, (2) non-readmitted and, (3) readmitted groups in boxplot for (a) LFP, (b) HFP, (c) TP and (d) pNN50. HRV feature values are highest in healthy group and lowest in the readmitted patient group. P-values obtained by two sample t-test demonstrate that each pair of the groups are significantly different.

It is evident from Fig. 6 that, compared to healthy subjects, HRV features decline in non-readmitted HF patients, then declines further in readmitted HF patients. This can also be due to cardiovascular autonomic imbalance as HRV is increased by parasympathetic nervous activation and decreased by sympathetic nervous system activation [54].

The following are some of the important takeaways from this research:

1. SCG can be used as a clinical tool in efficient management of HF patients. The current study demonstrates the potential use of SCG signal in HF readmission prediction.
2. In this study, the accuracies of conventional ML algorithms were higher than deep neural network (DNN) model. Other than adding the HRV features, an extensive dataset would benefit DNN model. Future analysis should include SCG signal in two other directions (lateral and caudocranial axes). Additionally, inclusion of 3-axis gyroscope sensor in the protocol would cover more complete cardiac movement by incorporating angular velocity of the heart. This can elicit more useful features related to HF readmission.
3. The advantage of using handcrafted features is the interpretability of the features. Extracting features based on physiological knowledge can make the results more meaningful and reveal underlying characteristics of the data. On the other hand, use of DNN model eliminated the need of manual feature engineering at the cost of interpretability. The future work of this study would be to focus on understanding the DNN model results by incorporating explainable AI techniques.
4. More patient data is required to confirm the current study results and apply in clinical settings.
5. The possibility that noncardiac comorbidities such as chronic kidney disease, diabetes, dementia etc. could be the cause of an HF readmission is one study limitation. SCG is limited to predict the readmissions associated with cardiac conditions.

V. CONCLUSION

This study describes a non-invasive technique to predict HF readmission. SCG, ECG, and GSR signals were acquired from non-readmitted and readmitted HF patients as well as normal subjects. After preprocessing and feature extraction, conventional ML algorithms and deep learning model were applied to classify the two patient groups. Results showed that KNN model achieved highest classification accuracy of about 90%. This suggests that SCG signal has potential utility for monitoring patients with cardiac disease. Early HF readmission prediction may potentially help the clinicians to identify the patients who need special care and treatment and make rapid targeted interventions to avoid readmission. This will ensure better management of HF patients and reduce the mortality rate. More patient populations with different cardiac conditions may be added for clinical application of SCG signal in future.

REFERENCES

- [1] G. Savarese and L. H. Lund, "Global Public Health Burden of Heart Failure," *Card. Fail. Rev.*, vol. 03, no. 01, p. 7, 2017, doi: 10.15420/cfr.2016:25:2.

- [2] S. S. Virani *et al.*, “Heart disease and stroke statistics—2020 update a report from the American Heart Association,” *Circulation*, vol. 141, no. 9, pp. E139–E596, 2020, doi: 10.1161/CIR.0000000000000757.
- [3] B. Bozkurt *et al.*, “Mortality, Outcomes, Costs, and Use of Medicines Following a First Heart Failure Hospitalization,” *JACC Heart Fail.*, Oct. 2023, doi: 10.1016/j.jchf.2023.04.017.
- [4] N. R. Jones, A. K. Roalfe, I. Adoki, F. D. R. Hobbs, and C. J. Taylor, “Survival of patients with chronic heart failure in the community: a systematic review and meta-analysis,” *Eur. J. Heart Fail.*, vol. 21, no. 11, pp. 1306–1325, Nov. 2019, doi: 10.1002/ejhf.1594.
- [5] W. Lesyuk, C. Kriza, and P. Kolominsky-Rabas, “Cost-of-illness studies in heart failure: A systematic review 2004-2016,” *BMC Cardiovasc. Disord.*, vol. 18, no. 1, May 2018, doi: 10.1186/s12872-018-0815-3.
- [6] P. A. Heidenreich *et al.*, “2022 AHA/ACC/HFSA Guideline for the Management of Heart Failure: A Report of the American College of Cardiology/American Heart Association Joint Committee on Clinical Practice Guidelines,” *Circulation*, vol. 145, no. 18, Lippincott Williams and Wilkins, pp. E895–E1032, May 2022. doi: 10.1161/CIR.0000000000001063.
- [7] M. Urbich *et al.*, “A Systematic Review of Medical Costs Associated with Heart Failure in the USA (2014–2020),” *PharmacoEconomics*, vol. 38, no. 11, Adis, pp. 1219–1236, Nov. 2020. doi: 10.1007/s40273-020-00952-0.
- [8] A. A. Shafie, Y. P. Tan, and C. H. Ng, “Systematic review of economic burden of heart failure,” *Heart Failure Reviews*, vol. 23, no. 1, Springer New York LLC, pp. 131–145, Jan. 2018. doi: 10.1007/s10741-017-9661-0.
- [9] M. S. Khan *et al.*, “Trends in 30- and 90-Day Readmission Rates for Heart Failure,” *Circ. Heart Fail.*, vol. 14, no. 4, p. E008335, Apr. 2021, doi: 10.1161/CIRCHEARTFAILURE.121.008335.
- [10] R. M. Lang *et al.*, “Recommendations for cardiac chamber quantification by echocardiography in adults: An update from the American Society of Echocardiography and the European Association of Cardiovascular Imaging,” *J. Am. Soc. Echocardiogr.*, vol. 28, no. 1, pp. 1-39.e14, 2015, doi: 10.1016/j.echo.2014.10.003.
- [11] S. P. Murphy, N. E. Ibrahim, and J. L. Januzzi, “Heart Failure with Reduced Ejection Fraction: A Review,” *JAMA - Journal of the American Medical Association*, vol. 324, no. 5, American Medical Association, pp. 488–504, Aug. 2020. doi: 10.1001/jama.2020.10262.
- [12] D. Burkhoff, “Mortality in heart failure with preserved ejection fraction: an unacceptably high rate.,” *European heart journal*, vol. 33, no. 14, pp. 1718–1720, Jul. 2012. doi: 10.1093/eurheartj/ehf339.
- [13] J. B. Somaratne, C. Berry, J. J. V. McMurray, K. K. Poppe, R. N. Doughty, and G. A. Whalley, “The prognostic significance of heart failure with preserved left ventricular ejection fraction: A literature-based meta-analysis,” *Eur. J. Heart Fail.*, vol. 11, no. 9, pp. 855–862, 2009, doi: 10.1093/eurjhf/hfp103.
- [14] X. Cui, E. Thunström, U. Dahlström, J. Zhou, J. Ge, and M. Fu, “Trends in cause-specific readmissions in heart failure with preserved vs. reduced and mid-range ejection fraction,” *ESC Heart Fail.*, vol. 7, no. 5, pp. 2894–2903, Oct. 2020, doi: 10.1002/ehf2.12899.
- [15] W. Sheikh *et al.*, “Association Between the Hospital Readmissions Reduction Program and Heart Failure Subtype Readmissions and Mortality in the USA,” *EMJ Cardiol.*, pp. 56–66, Oct. 2021, doi: 10.33590/emjcardiol/20-00285.
- [16] A. S. Desai and L. W. Stevenson, “Rehospitalization for heart failure: Predict or prevent?,” *Circulation*, vol. 126, no. 4, pp. 501–506, Jul. 2012, doi: 10.1161/CIRCULATIONAHA.112.125435.
- [17] B. D. Stauffer, “Effectiveness and Cost of a Transitional Care Program for Heart Failure: A Prospective Study With Concurrent Controls,” *Arch. Intern. Med.*, vol. 171, no. 14, p. 1238, Jul. 2011, doi: 10.1001/archinternmed.2011.274.
- [18] K. Shameer *et al.*, “PREDICTIVE MODELING OF HOSPITAL READMISSION RATES USING ELECTRONIC MEDICAL RECORD-WIDE MACHINE LEARNING: A CASE-STUDY USING MOUNT SINAI HEART FAILURE COHORT Sinai Health System at Mount Sinai 3 Decision Support, Mount Sinai Health System at Mount Sinai 4 Mount Sinai Data Warehouse, Icahn Institute of Genomics and Multiscale Biology at Mount Sinai HHS Public Access,” *Pac Symp Biocomput*, vol. 22, pp. 276–287, 2016. [Online]. Available: <https://www.cms.gov/>
- [19] S. E. Awan, M. Bennamoun, F. Sohel, F. M. Sanfilippo, and G. Dwivedi, “Machine learning-based prediction of heart failure readmission or death: implications of choosing the right model and the right metrics,” *ESC Heart Fail.*, vol. 6, no. 2, pp. 428–435, Apr. 2019, doi: 10.1002/ehf2.12419.
- [20] J. Liu, P. Liu, M.-R. Lei, H.-W. Zhang, A.-L. You, and X.-R. Luan, “Readmission Risk Prediction Model for Patients with Chronic Heart Failure: A Systematic Review and Meta-Analysis,” *Iran J Public Health*, vol. 51, no. 7, pp. 1481–1493, 2022. [Online]. Available: <http://ijph.tums.ac.ir>
- [21] J. G. F. Cleland and R. Antony, “It makes SENSE to take a safer road,” *European Heart Journal*, vol. 32, no. 18, pp. 2225–2227, Sep. 2011. doi: 10.1093/eurheartj/ehf120.
- [22] E. K. Heist *et al.*, “Analysis of different device-based intrathoracic impedance vectors for detection of heart failure events (from the detect fluid early from intrathoracic impedance monitoring study),” *Am. J. Cardiol.*, vol. 114, no. 8, pp. 1249–1256, Oct. 2014, doi: 10.1016/j.amjcard.2014.07.048.
- [23] J. Stehlik *et al.*, “Continuous Wearable Monitoring Analytics Predict Heart Failure Hospitalization: The LINK-HF Multicenter Study,” *Circ. Heart Fail.*, vol. 13, no. 3, p. E006513, Mar. 2020, doi: 10.1161/CIRCHEARTFAILURE.119.006513.

- [24] C. M. Yu *et al.*, “Intrathoracic impedance monitoring in patients with heart failure: Correlation with fluid status and feasibility of early warning preceding hospitalization,” *Circulation*, vol. 112, no. 6, pp. 841–848, Aug. 2005, doi: 10.1161/CIRCULATIONAHA.104.492207.
- [25] J. P. Boehmer *et al.*, “A Multisensor Algorithm Predicts Heart Failure Events in Patients With Implanted Devices Results From the MultiSENSE Study.” 2017.
- [26] W. Y. Lin, H. L. Ke, W. C. Chou, P. C. Chang, T. H. Tsai, and M. Y. Lee, “Realization and technology acceptance test of a wearable cardiac health monitoring and early warning system with multi-channel MCGs and ECG,” *Sens. Switz.*, vol. 18, no. 10, Oct. 2018, doi: 10.3390/s18103538.
- [27] O. T. Inan *et al.*, “Novel Wearable Seismocardiography and Machine Learning Algorithms Can Assess Clinical Status of Heart Failure Patients,” *Circ. Heart Fail.*, vol. 11, no. 1, p. e004313, Jan. 2018, doi: 10.1161/CIRCHEARTFAILURE.117.004313.
- [28] K. Azad, P. T. Gamage, R. H. Sandler, N. Raval, and H. A. Mansy, “Detection of respiratory phase and rate from chest surface measurements,” *J. Appl. Biotechnol. Bioeng.*, vol. 5, no. 6, pp. 359–362, 2018.
- [29] M. K. Azad, P. T. Gamage, R. Dhar, R. H. Sandler, and H. A. Mansy, “Postural and longitudinal variability in seismocardiographic signals,” *Physiol. Meas.*, vol. 44, no. 2, p. 025001, Feb. 2023, doi: 10.1088/1361-6579/acb30e.
- [30] P. T. Gamage, M. K. Azad, A. Taebi, R. H. Sandler, and H. A. Mansy, “Clustering of SCG Events Using Unsupervised Machine Learning,” in *Signal Processing in Medicine and Biology: Emerging Trends in Research and Applications*, Springer International Publishing, 2020, pp. 205–233. doi: 10.1007/978-3-030-36844-9_7.
- [31] M. K. Azad, P. T. Gamage, R. H. Sandler, N. Raval, and H. A. Mansy, “Seismocardiographic Signal Variability During Regular Breathing and Breath Hold in Healthy Adults,” in *2019 IEEE Signal Processing in Medicine and Biology Symposium (SPMB)*, Philadelphia, PA, USA: IEEE, Dec. 2019, pp. 1–7. doi: 10.1109/SPMB47826.2019.9037852.
- [32] R. H. Sandler *et al.*, “Minimizing Seismocardiography Variability by Accounting for Respiratory Effects,” *J. Card. Fail.*, vol. 25, no. 8, p. S185, Aug. 2019, doi: 10.1016/j.cardfail.2019.07.521.
- [33] Y. Guo, F.-L. Chung, G. Li, and L. Zhang, “Multi-Label Bioinformatics Data Classification With Ensemble Embedded Feature Selection,” *IEEE Access*, vol. 7, pp. 103863–103875, 2019, doi: 10.1109/ACCESS.2019.2931035.
- [34] N. Pudjihartono, T. Fadason, A. W. Kempa-Liehr, and J. M. O’Sullivan, “A Review of Feature Selection Methods for Machine Learning-Based Disease Risk Prediction,” *Front. Bioinforma.*, vol. 2, p. 927312, 2022, doi: 10.3389/fbinf.2022.927312.
- [35] X. Bao *et al.*, “Time-Frequency distributions of heart sound signals: A Comparative study using convolutional neural networks,” *Biomed. Eng. Adv.*, vol. 5, p. 100093, Jun. 2023, doi: 10.1016/j.bea.2023.100093.
- [36] A. Taebi and H. A. Mansy, “Time-Frequency Distribution of Seismocardiographic Signals: A Comparative Study,” *Bioeng. Basel Switz.*, vol. 4, no. 2, p. 32, Apr. 2017, doi: 10.3390/bioengineering4020032.
- [37] K. He, X. Zhang, S. Ren, and J. Sun, “Deep Residual Learning for Image Recognition,” 2015, doi: 10.48550/ARXIV.1512.03385.
- [38] A. Diker, Z. Comert, E. Avci, M. Togacar, and B. Ergen, “A Novel Application based on Spectrogram and Convolutional Neural Network for ECG Classification,” in *2019 1st International Informatics and Software Engineering Conference (UBMYK)*, Ankara, Turkey: IEEE, Nov. 2019, pp. 1–6. doi: 10.1109/UBMYK48245.2019.8965506.
- [39] Y. Zhang, J. Li, S. Wei, F. Zhou, and D. Li, “Heartbeats Classification Using Hybrid Time-Frequency Analysis and Transfer Learning Based on ResNet,” *IEEE J. Biomed. Health Inform.*, vol. 25, no. 11, pp. 4175–4184, Nov. 2021, doi: 10.1109/JBHI.2021.3085318.
- [40] J. S. Richman and J. R. Moorman, “Physiological time-series analysis using approximate entropy and sample entropy,” *Am. J. Physiol.-Heart Circ. Physiol.*, vol. 278, no. 6, pp. H2039–H2049, Jun. 2000, doi: 10.1152/ajpheart.2000.278.6.H2039.
- [41] T. Higuchi, “Approach to an irregular time series on the basis of the fractal theory,” *Phys. Nonlinear Phenom.*, vol. 31, no. 2, pp. 277–283, Jun. 1988, doi: 10.1016/0167-2789(88)90081-4.
- [42] P. F. Binkley, E. Nunziata, G. J. Haas, S. D. Nelson, and R. J. Cody, “Parasympathetic withdrawal is an integral component of autonomic imbalance in congestive heart failure: Demonstration in human subjects and verification in a paced canine model of ventricular failure,” *J. Am. Coll. Cardiol.*, vol. 18, no. 2, pp. 464–472, Aug. 1991, doi: 10.1016/0735-1097(91)90602-6.
- [43] E. Braunwald and M. R. Bristow, “Congestive Heart Failure: Fifty Years of Progress,” *Circulation*, vol. 102, no. suppl_4, Nov. 2000, doi: 10.1161/circ.102.suppl_4.IV-14.
- [44] J. S. Floras, “Sympathetic nervous system activation in human heart failure: clinical implications of an updated model,” *J. Am. Coll. Cardiol.*, vol. 54, no. 5, pp. 375–385, Jul. 2009, doi: 10.1016/j.jacc.2009.03.061.
- [45] D. L. Mann, “Mechanisms and models in heart failure: A combinatorial approach,” *Circulation*, vol. 100, no. 9, pp. 999–1008, Aug. 1999, doi: 10.1161/01.cir.100.9.999.
- [46] A. Roy, S. Guatimosim, V. F. Prado, R. Gros, and M. A. M. Prado, “Cholinergic Activity as a New Target in Diseases of the Heart,” *Mol. Med.*, vol. 20, no. 1, pp. 527–537, Jan. 2014, doi: 10.2119/molmed.2014.00125.
- [47] C. Sam and B. Bordoni, “Physiology, Acetylcholine,” in *StatPearls*, Treasure Island (FL): StatPearls Publishing, 2023. Accessed: Jan. 04, 2024. [Online]. Available: <http://www.ncbi.nlm.nih.gov/books/NBK557825/>
- [48] J. B. Galper and T. W. Smith, “Properties of muscarinic acetylcholine receptors in heart cell cultures,” *Proc. Natl. Acad. Sci.*, vol. 75, no. 12, pp. 5831–5835, Dec. 1978, doi: 10.1073/pnas.75.12.5831.

- [49] R. Moss, F. B. Sachse, E. G. Moreno-Galindo, R. A. Navarro-Polanco, M. Tristani-Firouzi, and G. Seemann, "Modeling effects of voltage dependent properties of the cardiac muscarinic receptor on human sinus node function," *PLoS Comput. Biol.*, vol. 14, no. 10, p. e1006438, Oct. 2018, doi: 10.1371/journal.pcbi.1006438.
- [50] I. Koncz *et al.*, "Acetylcholine Reduces IKr and Prolongs Action Potentials in Human Ventricular Cardiomyocytes," *Biomedicines*, vol. 10, no. 2, p. 244, Jan. 2022, doi: 10.3390/biomedicines10020244.
- [51] H. Ahammer *et al.*, "Sinoatrial Beat to Beat Variability Assessed by Contraction Strength in Addition to the Interbeat Interval," *Front. Physiol.*, vol. 9, p. 546, May 2018, doi: 10.3389/fphys.2018.00546.
- [52] M. D. Rienzo *et al.*, "Wearable seismocardiography: Towards a beat-by-beat assessment of cardiac mechanics in ambulant subjects," *Auton. Neurosci.*, vol. 178, no. 1–2, pp. 50–59, Nov. 2013, doi: 10.1016/j.autneu.2013.04.005.
- [53] A. Taebi, B. Solar, A. Bomar, R. Sandler, and H. Mansy, "Recent Advances in Seismocardiography," *Vibration*, vol. 2, no. 1, pp. 64–86, Jan. 2019, doi: 10.3390/vibration2010005.
- [54] G. G. Berntson *et al.*, "Heart rate variability: Origins, methods, and interpretive caveats," *Psychophysiology*, vol. 34, no. 6, pp. 623–648, Nov. 1997, doi: 10.1111/j.1469-8986.1997.tb02140.x.